Neuroscience Research 106 (2016) 12–22

Contents lists available at ScienceDirect

Neuroscience Research

journal homepage: www.elsevier.com/locate/neures

Analysis of RNA metabolism in peripheral WBCs of TDP-43 KI mice identifies novel biomarkers of ALS

Minami Hasegawa[a,b], Chikako Hara-Miyauchi[a,b], Hiroki Ohta[a,c], Kenji Sakimura[d], Hideyuki Okano[b,**], Hirotaka James Okano[a,b,*]

[a] Division of Regenerative Medicine, Jikei University School of Medicine, 3-25-8 Nishi-Shimbashi, Minato-ku, Tokyo 1058461, Japan
[b] Department of Physiology, Keio University School of Medicine, 35 Shinanomachi, Shinjuku-ku, Tokyo 160-8582, Japan
[c] Vascular Surgery, Department of Surgery, Jikei University School of Medicine, 3-25-8 Nishi-Shimbashi, Minato-ku, Tokyo 1058461, Japan
[d] Department of Cellular Neurobiology, Brain Research Institute, Niigata University, 1-757 Asahimachidori Niigata Chuo-ku, Niigata 951-8585, Japan

ARTICLE INFO

Article history:
Received 21 October 2015
Received in revised form
25 November 2015
Accepted 27 November 2015
Available online 7 December 2015

Keywords:
ALS
Biomarker
TDP-43
RNA metabolism
Peripheral blood cells

ABSTRACT

Diagnostic biomarkers for amyotrophic lateral sclerosis (ALS) have yet to be identified. One of the causes of neuronal cell death in neurodegenerative diseases is abnormal RNA metabolism, although the mechanisms by which this occurs are unclear. Detection of abnormal RNA metabolism in white blood cells (WBCs) could lead to a new biomarker of ALS onset. TAR DNA-binding protein 43 kDa (TDP-43) is *an* RNA-binding protein that regulates RNA metabolism. We previously developed a mouse model of ALS that exhibits adult-onset motor dysfunction; these mutant TDP-43 knock in (KI) mice heterozygously express mutant human TDP-43 (A382T or G348C). In the present study, we examined TDP-43 mRNA levels in WBCs of KI mice and found that A382T mutant mRNA is significantly higher than G348C. Our results suggest that each mutant TDP-43 induces distinct RNA metabolism, and that the expression of total TDP-43 alone in WBC is not suitable as an ALS biomarker. To identify additional candidates, we focused on survival and apoptosis-related factors and examined their mRNA metabolism in WBCs. *mRNA levels of both Smn1 and Naip*5 correlated with TDP-43 levels and also differed between A382T and G348C. Together, TDP-43 and these factors may enable detection of abnormalities in individual ALS pathologies.

1. Introduction

Amyotrophic lateral sclerosis (ALS) is a neurodegenerative disease that selectively affects motor neurons (MNs) and leads to a progressive loss of motor function, paralysis, and death. In most cases, ALS is an adult-onset disease, and patients develop respiratory failure within 3–5 years of diagnosis (Rowland and Shneider, 2001). There are no effective cures for ALS, but riluzole has been shown to delay progression and prolong survival by an average of 3 months (Rowland et al., 2001). Although the majority of ALS cases are sporadic (sALS), approximately 10% are familial (fALS) (Rowland and Shneider, 2001). In familial cases, gene mutations have been identified at many ALS-associated gene loci (Kwiatkowski et al., 2009; Deng et al., 2011; Renton et al., 2011; Wu et al., 2012). For example, more than 20 years ago, the Cu/Zn superoxide dismutase 1 (SOD1) gene was identified as being responsible for familial ALS for the first time (Rosen et al., 1993).

In ALS, the accumulation of abnormal proteins in affected MNs is a neuropathological hallmark. The TARDNA binding protein 43 (TDP-43) is a major component of ubiquitin-positive neuronal inclusions in both ALS and frontotemporal dementia. Normally, TDP-43 localizes in cell nuclei; however, in ALS MNs it is found in the cytoplasm (Arai et al., 2006; Neumann et al., 2006). The pathological mutations responsible for ALS are mainly found in the TDP-43 C-terminal domain, which contains highly conserved glycine-rich regions (Gitcho et al., 2008; Kabashi et al., 2008; Sreedharan et al., 2008; Yokoseki et al., 2008). Mutations in TDP-43 account for approximately 4% of fALS and a smaller percentage of sALS (Chiò et al., 2012).

Recently, it has been proposed that RNA metabolism is related to MN degeneration. In fact, half of the genes responsible for fALS have been found to be associated with RNA metabolism (Droppelmann et al., 2014). TDP-43 is *an* RNA-binding protein that regulates metabolism of target RNA, pre-mRNA splicing, mRNA stability, and

* Corresponding author at: 3-25-8 Nishi-Shimbashi, Minato-ku, Tokyo 1058461, Japan. Tel.: +81 3 3433 1111/3 5400 1200x2350; fax: +81 3 5400 1297.
** Corresponding author at: 35 Shinanomachi, Shinjuku-ku, Tokyo 160-8582, Japan. Tel.: +81 3 5363 3747; fax: +81 3 3357 5445.
E-mail addresses: hidokano@a2.keio.jp (H. Okano), hjokano@jikei.ac.jp (H.J. Okano).

http://dx.doi.org/10.1016/j.neures.2015.11.009

transport (Buratti et al., 2001). Previously, we used two TDP-43 mutations, A382T and G348C, to produce mutant TDP-43 knock-in (KI) mice as an ALS model. These mice show poor weight gain and gradually exhibit adult-onset motor dysfunction from seven months of age, making them a useful model for pathological analysis of symptom progression.

There are no biomarkers of MN degeneration, and thus diagnosis of ALS still depends on clinical symptoms (Valadi, 2015). Consequently, there is a pronounced delay between symptom onset and diagnosis. Furthermore, long delays in diagnosis mean that treatment for the progressing disease often occurs too late to be optimally effective. Various techniques have been proposed to identify biomarkers, including diagnostic magnetic resonance imaging of the brain or spinal cord, although it is difficult to identify patients at risk in the non-symptomatic stage of ALS (Pradat and El Mendili, 2014). Another method consists of performing proteasome analysis of the cerebrospinal fluid (CSF) of ALS patients (Tarasiuk et al., 2012); however, this approach is invasive and can be painful. Thus, in the present study, we searched for ALS biomarkers using peripheral blood cells of mutant TDP-43 KI mice. We hypothesize that abnormal RNA metabolism related to TDP-43 mutants may serve as a useful biomarker for the assessment of ALS progression. We investigate the expression and mRNA levels of TDP-43, as well as shifts in mRNA levels of survival and apoptosis-related factors in white blood cells (WBCs) of KI mice.

2. Experimental procedures

2.1. Animals

Experimental procedures and housing conditions for animals were approved by the Jikei University Animal Ethics Committees (approval number, 24-019). The mutant TDP-43 KI mice had human TDP-43, including C-terminal point mutations of amino acids fused with Venus, Ala to Thr in 382 (A382T) or Gly to Cys in 348 (G348C). Details on the genetic development and behavioral and pathological analysis of these two KI mice will be described in a separate report, now in preparation.

2.2. Peripheral blood and organ collection

The mice were anesthetized using isoflurane (Pfizer, New York, NY, USA), and peripheral blood cells were collected from their hearts using a 26-G needle and 1 mL heparinized syringe. Blood samples were treated for each experiment. The heart, lung, liver, spinal cord, and brain were collected, and RNA isolations were immediately performed.

2.3. siRNAs

siDirect 2.0 software was used to design novel siRNAs (Fig. S1). Three siRNAs were designed for the 3′-UTR sequence of mouse TDP-43. There is no 3′-UTR sequence in mutant human TDP-43::Venus, and the KI gene was not silenced by siRNAs for mouse TDP-43. We selected a siRNA exhibiting a high silencing effect from these three candidates (Fig. S2). KI gene silencing was targeted to Venus sequences (Fig. S1). Total TDP-43 gene silencing was performed using mixtures of each volume of mouse TDP-43 siRNA and Venus siRNA. The siRNA sequences were described in supplementary method.

2.4. Antibodies

The following antibodies were used for western blotting: Anti-TDP-43 (Proteintech, Chicago, IL, USA), 1:1000; anti-GFP (MBL, Nagoya, Japan), 1:1000; β-actin (Sigma, St. Louis, MO, USA), 1:2000; horseradish peroxidase (HRP)-conjugated goat anti-rabbit (Millipore, Darmstadt, Germany), and goat anti-mouse (Millipore), 1:2000. For immunocytochemistry, anti-TDP-43, anti-GFP, goat anti-mouse Alexa 633 (Molecular Probes, Eugene, OR, USA), and goat anti-rabbit Alexa 647 (Molecular Probes) were used at 1:100. Hoechst33342 (Molecular Probes) was used at 1:100,000,000.

2.5. Cell culture and transfection

Astrocytes were isolated from the brain cortices of P1 mutant TDP-43 KI mice. The cells were maintained in high-glucose DMEM (SIGMA) with 20% heat-inactivated fetal bovine serum (Thermo Scientific, Waltham, MA, USA) and 100 μg/mL penicillin–streptomycin solution (Wako, Osaka, Japan). siRNAs were transfected into cells using Lipofectamine®RNAi MAX Reagent (Invitrogen, Carlsbad, CA, USA). After 48 h in culture, the cells were collected and used in a protein isolation step.

2.6. RNA isolations and real-time RT-PCR

Total RNA was extracted from each organ of the mice using TRIzol® reagent (Invitrogen) and RNeasy® Plus Mini Kit (Qiagen, Hilden, Germany). For real-time RT-PCR, first-strand cDNA synthesis was performed using the PrimeScript® RT Master Mix (Takara Bio, Shiga, Japan) following the manufacturer's protocol. Real-time RT-PCR was performed using a TaqMan® Gene Expression Assay Master Mix (Applied Biosystems, Foster City, CA, USA) with an ABI 7300 Real-time PCR system (Applied Biosystems). The mRNA levels in the samples were normalized using beta-actin. For RT-PCR, first-strand cDNAs were synthesized using ReverTra Ace α (TOYOBO, Osaka, Japan), according to the manufacturer's protocol. PCR amplification was performed using KOD plus enzyme. TaqMan® MGB probes, primers and amplification conditions were described in supplementary method.

2.7. Protein extraction

Protein extraction from cultured astrocytes was performed using mixture of Complete Mini (Roche Basel, Switzerland) and Tissue Extraction Reagent I (Invitrogen) containing 50 mM Tris (pH 7.4), 250 mM NaCl, 5 mM EDTA, 2 mM Na_3VO_4, 1 mM NaF, 20 mM $Na_4P_2O_7$, and 0.02% NaN_3 was added into each culture well. After intense dissociation, the extracts were incubated for 5 min on ice. Centrifugation was performed at 20,000 × *g* for 15 min, and the lysates were stored at −80 °C.

2.8. Western blotting

Samples were diluted with equal volumes of Laemmli Sample Buffer (Bio Rad, Hercules, CA, USA) containing 62.5 mM Tris-HCl (pH 6.8), 25% glycerol, 2% SDS, 0.01% Bromophenol Blue, and 5% 2-mercaptoethanol, then incubated for 3 min at 95 °C. Protein samples were separated using SDS-PAGE and transferred to polyvinylidene difluoride membranes (Millipore). The membranes were blocked with 1% non-fat skim milk for 30 min at room temperature (RT) and incubated in primary antibody solutions for 16 h at 4 °C. Thereafter, the membranes were incubated with secondary antibodies for 2 h at RT. Signals were detected using Chemiluminescence HRP Substrate (Takara Bio) with a LAS3000 Mini (FUJI FILM, Tokyo, Japan). Semi-quantitative analysis of the signals was performed using ImageJ software (National Institute of Health).

2.9. Immunocytochemistry

Whole blood cells were fixed in 4% paraformaldehyde solution for 3 min at RTHemolyzed red blood cells were removed by PBS wash, and the cells were incubated in 5% bovine serum albumin/PBS solution for 1 h at RT. Primary antibody was dissolved in blocking solution, and the cells were incubated for 1 h at RT, and then, incubated in secondary antibody solution 1 h at RT. The cells were dissociated in PBS containing 0.05% NaN_3 and enclosed under a coverslip. Microscopy was performed using a fluorescence microscope (IX73; Olympus, Tokyo, Japan) equipped with an objective lens (UPlanSApo 60× N.A. = 1.35; Olympus), a 0.5× zoom lens (Olympus) and a charge-coupled device camera (Cool SNAP EZ; Photometrics, Tucson, AZ, USA). The microscope was driven by MetaView software. The photographic conditions were described in supplementary method.

2.10. Fluorescence microscopy condition and image analysis

Lymphocytes which selected by cell size less than 30 μm^2 were imaged by fluorescent microscopy (Olympus, IX73). The deviation was calculated by measuring pixel intensity of each cell. High deviation produced and kept the localization of TDP-43 as high non-uniformity. Details of photographic conditions were described in supplementary methods.

2.11. Statistical analysis

Statistical significance was determined using the unpaired *t*-test as detailed in the figure legends.

3. Results

3.1. Mutant TDP-43 mRNA was ubiquitously expressed in mutant TDP-43 KI mice

In our experiment, we use mutant TDP-43 KI mice exhibited late-onset motor dysfunction and poor weight gain, although manuscript about development of this mice *is* in preparation. These mice had mutant human TDP-43 (A382T or G348C) fused with Venus, and the transgene cut into exon 2 of the mouse *Tardbp* genome (Fig. 1A). In these KI mice, the transgene was expressed heterozygously due to the dominant heredity of the mutant TDP-43 gene. In addition, it was possible to detect wild type (WT) mouse TDP-43 and the KI gene separately by targeting Venus as a reporter. We performed RT-PCR analysis in multiple organs, including heart, lung, liver, spinal cord, brain, and WBCs in TDP-43 (A382T) KI mice at the symptomatic stage. Mutant TDP-43 mRNA was ubiquitously expressed in each tissue (Fig. 1B). We also analyzed mRNA expression patterns of WT mouse TDP-43 and found that they also were ubiquitously expressed (data not shown).

3.2. The ratio of mutant TDP-43 increased in glial cells of A382T mutant mice relative to that in G348C mutants

We first investigated expression patterns of TDP-43 in the central nervous system (CNS) using primary cultured astrocytes collected from TDP-43 KI mice. Western blotting was carried out to separately detect expression of mouse and mutant human TDP-43. Anti-TDP-43 antibody detected WT mouse TDP-43 (43 kDa) and mutant human TDP-43::Venus (70 kDa; Fig. 2A and C). Protein expression derived from the transgene was also detected by anti-GFP antibody (70 kDa; Fig. 2A and D). WT mouse TDP-43 expression level was decreased by half in A382T cells relative to that in WT astrocytes (Fig. 2C). The change in mutant TDP-43 expression level detected by the anti-GFP antibody was not significant, but

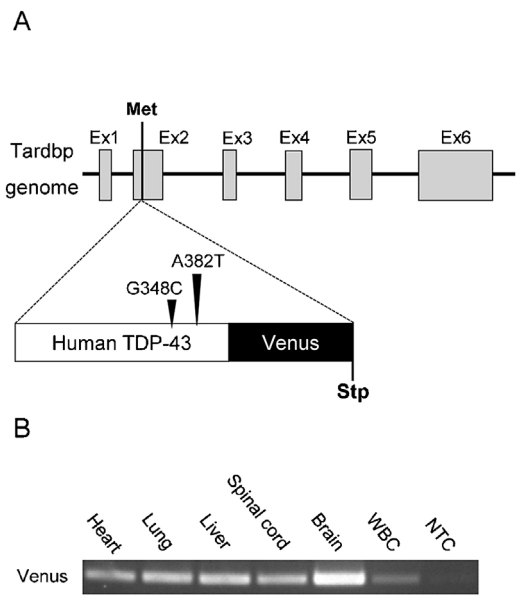

Fig. 1. Mutant TDP-43 is expressed in various tissues of mutant TDP-43 KI mice. (A) Schematic representation of the domain architecture of the transgene. Filled boxes and lines represent exons (Ex) or introns of the *Tardbp* genome, respectively. The mice express human mutant TDP-43::Venus, which has TDP-43 point mutations in amino acids A382T and G348C. The transgene cut into exon2 of mouse *Tardbp*. Met, methionine residue; Stp, stop codon. (B) mRNA expression of the transgene in various organs of TDP-43 (A382T) KI mice aged 10 months. Transgene detections were performed by designing primers that bound Venus sequences. Mutant TDP-43 was ubiquitously expressed in the mice. NTC, non-template control.

tended to increase in A382T astrocytes, which corresponded to the results from anti-TDP-43 antibody detection (Fig. 2D). In astrocytes carrying each mutation, no significant difference in total TDP-43 expression levels were observed (Fig. 2B), but the ratio of mutant TDP-43 expression was two-fold higher in A382T astrocytes relative to those in G348C astrocytes (Fig. 2E). Our data thus suggest that in the CNS of KI mice, the metabolism of TDP-43 in mutant A382T and G348C differs.

3.3. Mutant TDP-43 can be also involved in negative feedback loop of autoregulation

To elucidate the regulation mechanisms of mouse and mutant human TDP-43 expression in KI mice, knock-down (KD) experiments were performed in KI astrocytes using siRNAs (Fig. 3). We demonstrated individual silencing in mouse and (or) mutant TDP-43 and analyzed the responsivity of expression in each. The siRNA designs are described in Fig. S1. Mutant human TDP-43 KD was performed by targeting sequences of Venus. For WT mouse TDP-43 KD, we designed three siRNAs that bound to 3′UTR and selected siRNA 3 (Fig. S2). A mouse and mutant humanTDP-43 siRNA mixture was used for total TDP-43 KD. In the two mutant astrocytes, an approximate 1.5-fold increment of WT mouse TDP-43 was induced by mutant human TDP-43 silencing. Conversely, mutant human TDP-43 expression levels were not affected by WT mouse TDP-43 KD (Fig. 3A, C, E and G). Moreover, the total TDP-43 expression levels were complemented by WT mouse TDP-43 upregulation induced by mutant human TDP-43 KD (Fig. 3B and F). Expression and localization patterns of mutant human TDP-43, detected by the anti-TDP-43 antibody corresponded to those from the anti-GFP antibody (Fig. 3D and H). We did not detect a significant difference in self-regulation between A382T and G348C. At least, WT TDP-43 encoding mRNA, but not human mutant TDP-43 encoding mRNA, is regulated by both WT and mutant TDP-43 through the 3′UTR.

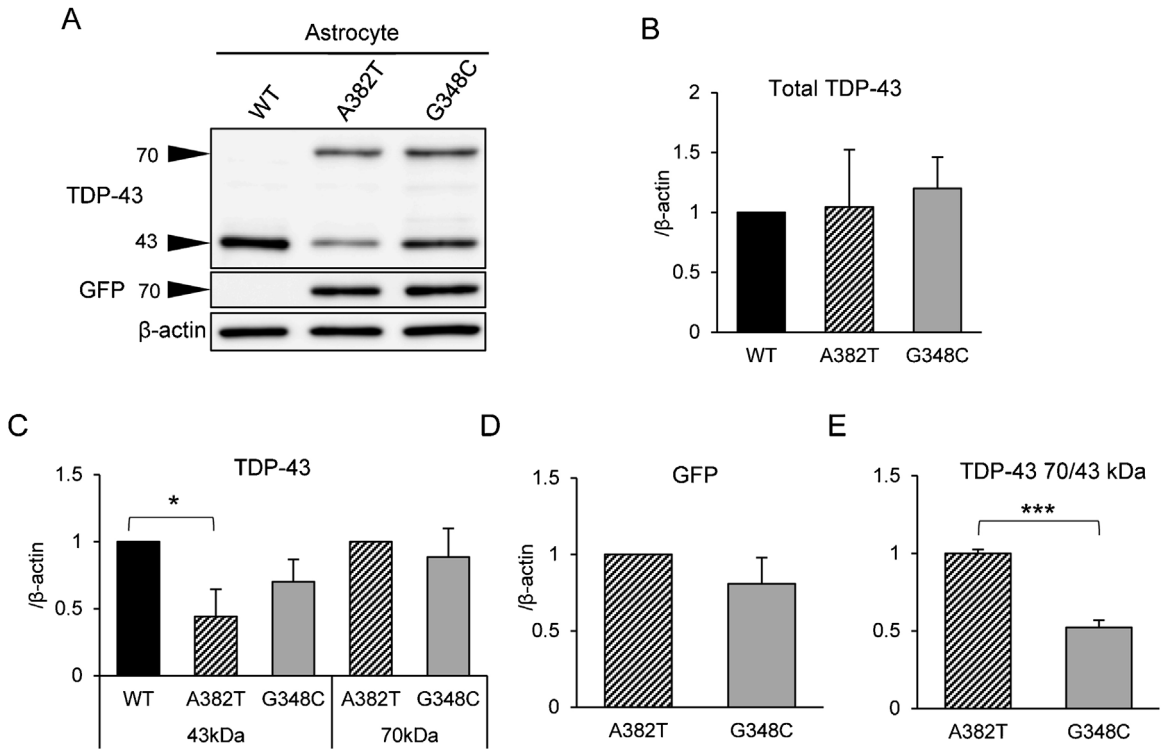

Fig. 2. Expression of TDP-43 is different between two types of mutant TDP-43 KI mice in cultured astrocytes. (A) Western blotting of TDP-43 expression in primary cultured astrocytes from mutant TDP-43 KI mice. Anti-TDP-43 antibodies were used to detect WT mouse TDP-43 (43 kDa) and mutant TDP-43::Venus (70 kDa). Venus fused TDP-43 protein was also detected by an antibody against GFP (70 kDa). (B–E) Quantitative analysis of each band detected by anti-TDP-43 (B, C) and anti-GFP antibodies (D). In (B), the sum of the 43 and 70 kDa bands data were considered to be the expression levels of total TDP-43. In (C), WT mouse TDP-43 (43 kDa) was decreased in A382T relative to that in WT [A382T, 0.44 (SD = 0.205) relative to WT ($p = 0.04$)]. (E) Expression ratio of mutant and WT mouse TDP-43 [G348C, 0.522 (SD = 0.046) relative to A382T ($p = 0.00009$)]. $N = 3$ of each genotype. Quantitative analysis was performed using ImageJ software. Data were analyzed using an unpaired t-test ($^{*}p < 0.05$, $^{**}p < 0.01$).

3.4. Mutant and normal TDP-43 were detected individually in WBCs of mutant TDP-43 KI mice

To investigate whether the differences between A382T and G348C also occurred in WBCs of KI mice, we attempted to individually detect expression of mutant and WT mouse TDP-43 by WBCs immunocytochemistry. These TDP-43 KI mice showed motor dysfunction at seven months (Hara-Miyauchi et al., in preparation), and so we performed experiments using mice aged four months, which we considered to be a presymptomatic stage. Mutant human TDP-43 expression was detected by anti-GFP antibody or fluorescence of Venus, and the signals were predominantly merged in the nucleus (Fig. 4A). Localization of mutant human and WT mouse TDP-43 were detected by anti-TDP-43 antibody (Fig. 4B). In the WT mice WBCs, Venus fluorescence was not observed, but TDP-43 expression was detected by anti-TDP-43 antibody (Fig. 4B). Corresponding to mutant TDP-43 protein, the signals detected by the antibody were mainly observed in the nucleus.

3.5. Expression of TDP-43 also changed in WBCs between the two mutant mice

We focused on TDP-43 expression in WBCs and performed fluorescence intensity analysis. Using ImageJ software, we selected lymphocytes by cell size and nucleus morphology (Fig. S3A and B). Before selection, the standard deviation (SD) of the cell size increased, and after the selection, the dispersion was minimized (Fig. S3A and B). Thereafter, we analyzed the fluorescence intensity of total or mutant TDP-43 signals in WBCs at the age of four (presymptomatic) and seven (symptomatic stage) months (Fig. 5). Total TDP-43 signals detected by the anti-TDP-43 antibody increased more than two-fold in A382T relative to those in WT and G348C at four months of age (Fig. 5A). At seven months, the signals also tended to increase, although the number of statistically significant differences decreased (Fig. 5A). The fluorescence intensities of mutant TDP-43::Venus increased 1.8-fold in A382T mutant mice in the presymptomatic stage and symptomatic stage (Fig. 5B). And in G348C, significant increase was observed in symptomatic stage than presymptomatic stage (Fig. 5A and B). In contrast to G348C, significant decrease between the stages was detected in total TDP-43 of A382T mice (Fig. 5A). Furthermore, we scored correlations between expression and non-uniformity of TDP-43 signals (Fig. 5C–F). We defined deviation in the fluorescence intensity of each cell as non-uniformity. In the presymptomatic stage, the fluorescence intensity and non-uniformity of total and mutant TDP-43 tended to increase in A382T (Fig. 5C and E). In the symptomatic stage, the total TDP-43 signals and dispersion also increased in A382T, which corresponded to the mutant TDP-43 signals (Fig. 5D and F). The results from staining intensity were consistent with the fluorescence intensity results, suggesting that stainability did not influence the expression analysis. Collectively, our results indicate that expression changes in TDP-43 occurred in WBCs of KI mice and that the degree of change varied between TDP-43 with different mutational positions.

3.6. mRNA metabolism of TDP-43 was altered in WBCs of mutant TDP-43 KI mice

It has recently been suggested that RNA metabolism, including RNA splicing, stability, and degradation, may be related to MN degeneration. Therefore, we hypothesized that abnormal RNA metabolism related to TDP-43 occurred in WBCs. To assess TDP-43 mRNA expression in mutant TDP-43 KI mice, real-time RT-PCR analysis was performed using TaqMan® MGB probes (Fig. 6). The

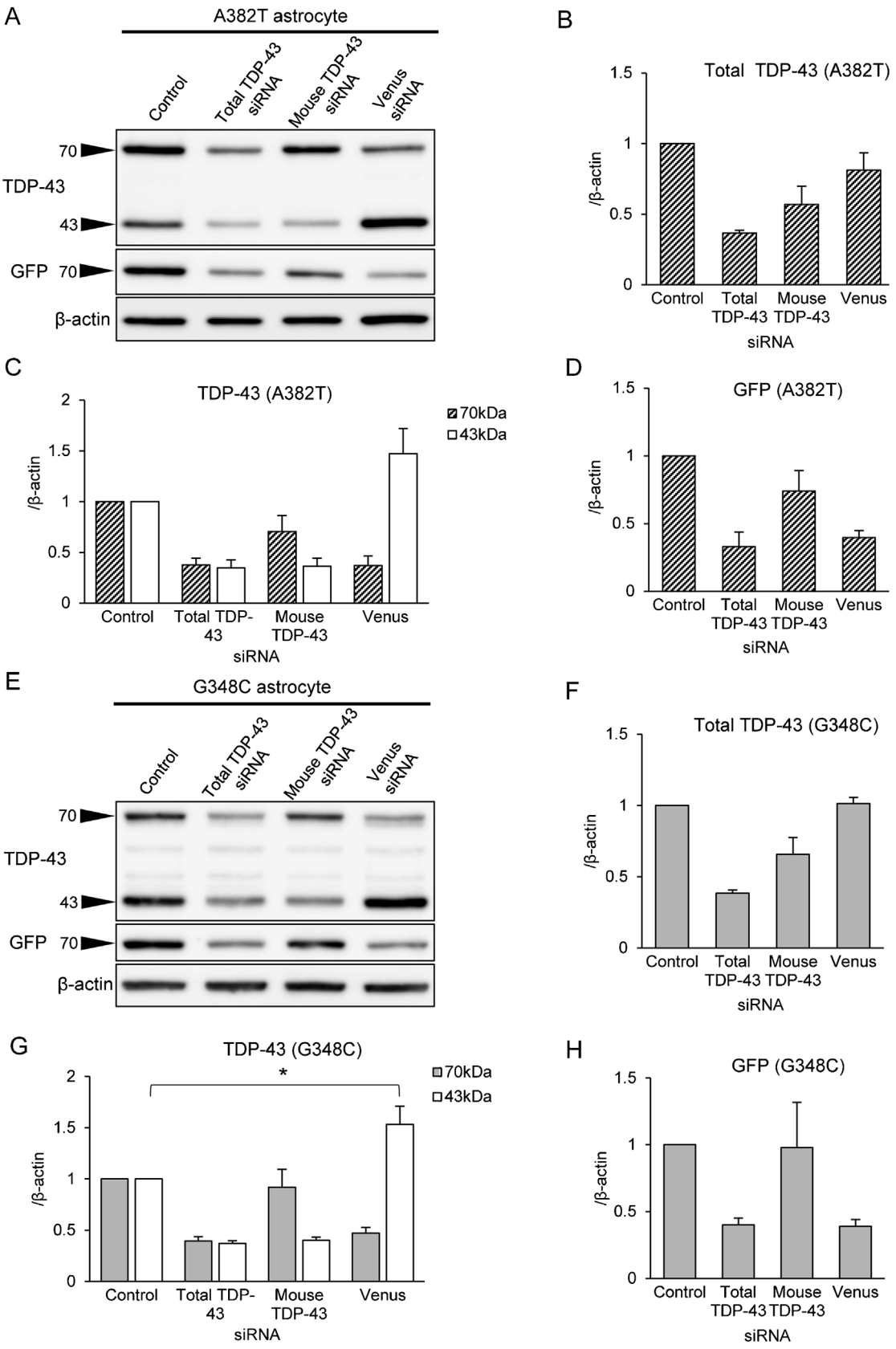

Fig. 3. Total TDP-43 expression level is regulated only by WT mouse TDP-43 in cultured astrocytes of the KI mice. (A, E) Western blotting of cultured astrocytes showed that TDP-43 expression was silenced by siRNA. (B–D, F–H) Quantitative analysis of expression levels were detected by different antibodies. (A–D) A382T and (E–H) G348C. Mouse TDP-43 siRNA was designed in the 3′-UTR in mouse TDP-43 mRNA, which led to KD of WT mouse TDP-43 only and not mutant human TDP-43. Mutant TDP-43::Venus was silenced by targeting mRNA of Venus. Total TDP-43 KD was performed using a mixture of mouse TDP-43 and Venus siRNA. KD experiments were performed three times for each genotype. In (C) and (G), increases in WT mouse TDP-43 expression levels were induced by mutant TDP-43 KD. A382T, 1.47 (SD = 0.25), $p > 0.05$; and G348C, 1.53 (SD = 0.18), $p = 0.03$ relative to control. Data were analyzed using an unpaired *t*-test ($^*p < 0.05$).

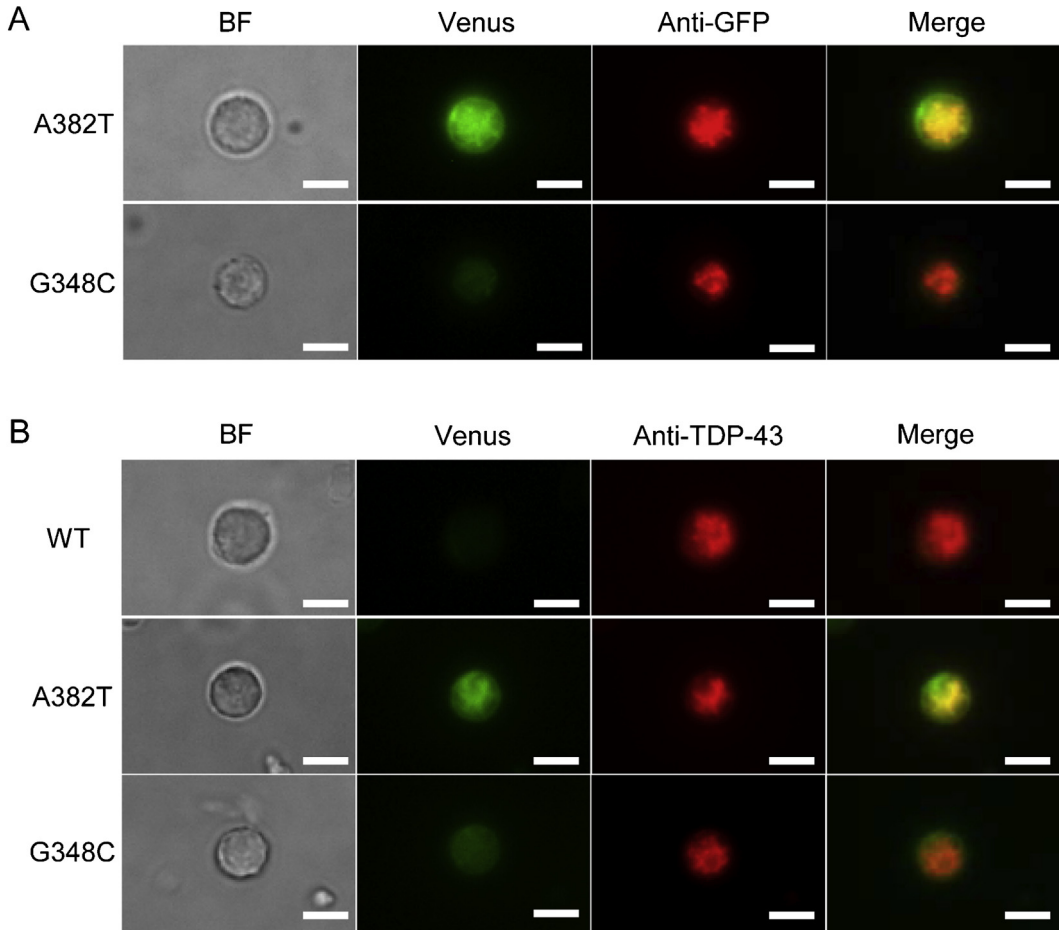

Fig. 4. Individual visualization of mutant and normal TDP-43 localization in WBCs of mutant TDP-43 KI mice. (A, B) Immunocytochemical analysis of mutant TDP-43 KI mouse WBCs at 4 months of age. Mutant TDP-43 expression was detected by fluorescence of Venus (A, B) and anti-GFP antibody (A). (B) Total TDP-43 expression was detected by anti-TDP-43 antibody. BF, Bright field, Scale bar, 5 μM.

TaqMan® designs are described in Supplementary Fig. 4. Total TDP-43 mRNA was detected by targeting the homologous domains of mouse TDP-43 and transgene allele. Notably, the mRNA expression level of total TDP-43 was significantly decreased in G348C mutant mice WBCs relative to those in A382T and WT (Fig. 6A). In addition, the mRNA expression patterns of mutant TDP-43 were also different between the A382T and G348C mutant mice (Fig. 6B). We also examined mRNA levels of total, mutant and mouse TDP-43 in brain cortex of the KI mice and the result indicated that mRNA level of mouse TDP-43 was significantly lower in A382T than G348C KI mice (Fig. S5). Overall, these data suggest that mRNA metabolism differs in KI mice carrying A382T or G348C mutations of TDP-43.

3.7. mRNA metabolism of MN survival and anti-apoptotic factors changed in WBCs of mutant TDP-43 KI mice

Our data suggest that RNA metabolism varies in different types of mutant TDP-43 KI mice. Thus, in ALS, RNA metabolism may be individually distinct. To study this, we used a combination of neurodegeneration-related factors, including TDP-43. Using survival motor neuron1 (Smn1) and neuronal apoptosis inhibitory protein (Naip), we performed mRNA expression analysis. The mRNA expression pattern of Smn1 was similar to that of total TDP-43 (Fig. 6C). In the mouse, seven genes that are highly homologous with Naip have been found, and four of them, including Naip1, 2, 5, and 6, have been reported to have transcripts (Diez et al., 2003). We used RT-PCR and sequence analysis to show that Naip5 was predominantly expressed in WBCs of KI mice (data not shown). The mRNA expression pattern of Naip5 showed an inverse correlation with that of total TDP-43 and Smn1 (Fig. 6D). In addition, we analyzed the mRNA expression level of a Naip5 splice variant. By performing RT-PCR and sequence analysis, we identified the exon 11 skipping splice variant of Naip5 in the KI mice WBCs. Although no reports have described a role of splice variants, we hypothesized that accumulation of abnormal splice variants occurred in KI mice WBCs. The mRNA expression pattern of an exon skipping variant of Naip5 was similar to that of total Naip5, in other words, we failed to detect abnormal splice variants of Naip5 (Fig. 6E). However, this concept may apply to unknown factors that are related to aberrant RNA metabolism. These results show that a combination of MN degeneration-related factors may enable determination of RNA metabolism in individual ALS patients.

4. Discussion

In the present study, TDP-43 RNA metabolism in the CNS and peripheral blood varied between two different types of mutant TDP-43 mice, and MN degeneration-related factors appeared to correlate with these differences. Detection of RNA metabolism in peripheral blood may thus reflect abnormalities in the CNS. Regarding TDP-43 metabolism, protein aggregation mechanisms have been discussed extensively in previous reports (Arai et al., 2006; Neumann et al., 2006; Kabashi et al., 2008; Swarup et al., 2011; Xiao et al., 2015). However, few studies have compared mutant TDP-43 function at the whole-body level.

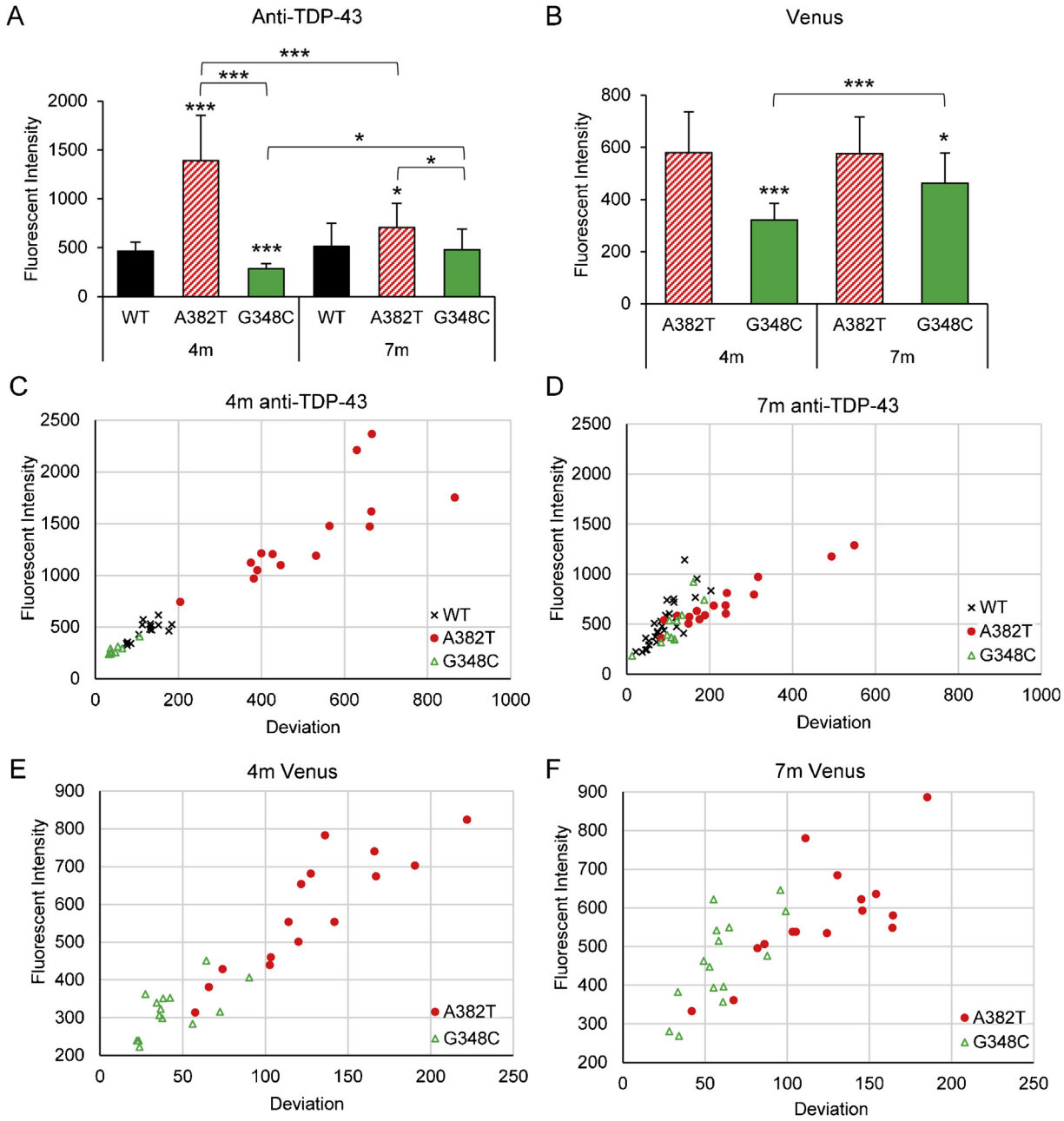

Fig. 5. Fluorescence intensity analysis of WBC images from mutant TDP-43 KI mice. (A, B) Fluorescence intensity quantification of total TDP-43 (A) or mutant TDP-43::Venus (B) in WBCs of the mice at the age of 4 and 7 months. (A) At 4 months: WT, 465.59 (SD = 90.48); A382T, 1390.40 (SD = 464.02); G348C, 284.27 (SD = 52.39); $p = 0.000004$ (A382T) and $p = 0.00002$ (G348C) compared with WT, and $p = 0.0000006$ for the comparison between A382T and G348C. At 7 months: WT, 515.02 (SD = 235.11); A382, 707.16 (SD = 248.18); G348C, 478.94 (SD = 212.93); $p = 0.015$ (A382T) and $p > 0.05$ (G348C) compared with WT, and $p = 0.020$ for the comparison between A382T and G348C. $N = 15$, 14, and 9 at 4 months; $n = 27$, 16, and 11 at 7 months for each genotype. (B) At 4 months: A382T, 578.41 (SD = 156.19); G348C; 321.14 (SD = 64.02); $p = 0.00001$. At 7 months: A382T, 575.89 (SD = 140.81); G348C; 462.45 (SD = 116.44); $p = 0.03$. $N = 15$ and 14 at 4 months; $n = 15$ and 15 at 7 months for each genotype. Data were analyzed using an unpaired t-test ($^{*}p < 0.05$, $^{***}p < 0.001$). (C–F) Correlation between fluorescence intensity and deviation of total TDP-43 signals detected by anti-TDP-43 antibody (C, D) or Venus signals (E, F) in cells of mice at age 4 (C, E) and 7 (D, F) months. Deviation of fluorescence intensity was considered to be a non-uniformity of mutant TDP-43 localization. The analysis of fluorescence intensity was performed using ImageJ software. $N = 15$, 14, and 9 at 4 months; $n = 13$, 16, and 11 at 7 months of each genotype.

Most investigations using animal models have been conducted on transgenic animals, and as such, TDP-43 was designed to be overexpressed using optional promoters and thus does not reflect physiological conditions. In our study, mice with mutant human TDP-43 knocked in were used. Similar to ALS patients, in heterozygous human TDP-43 KI mice, the transgene was expressed using the endogenous TDP-43 promoter. Therefore, for the first time, these experimental conditions enabled the physiological examination of TDP-43 expression. Furthermore, the Venus reporter gene was fused to TDP-43, allowing individual expression analysis of normal and mutant TDP-43. Using these mice, we show the ratio of TDP-43 (with either the A382T or G348C mutation) levels in the CNS. In previous studies, the two mutant human TDP-43 proteins were found to have long half-lives, and patients with these mutations tended to have juvenile-onset disease (Kabashi et al., 2008; Corrado et al., 2009; Watanabe et al., 2013). Regarding differences between mutants, a decrease in G348C mutant protein expression in cultured MNs has been reported (Kabashi et al., 2010). Consistent with these findings, we observed that mutant human TDP-43 was expressed at higher levels in A382T than in

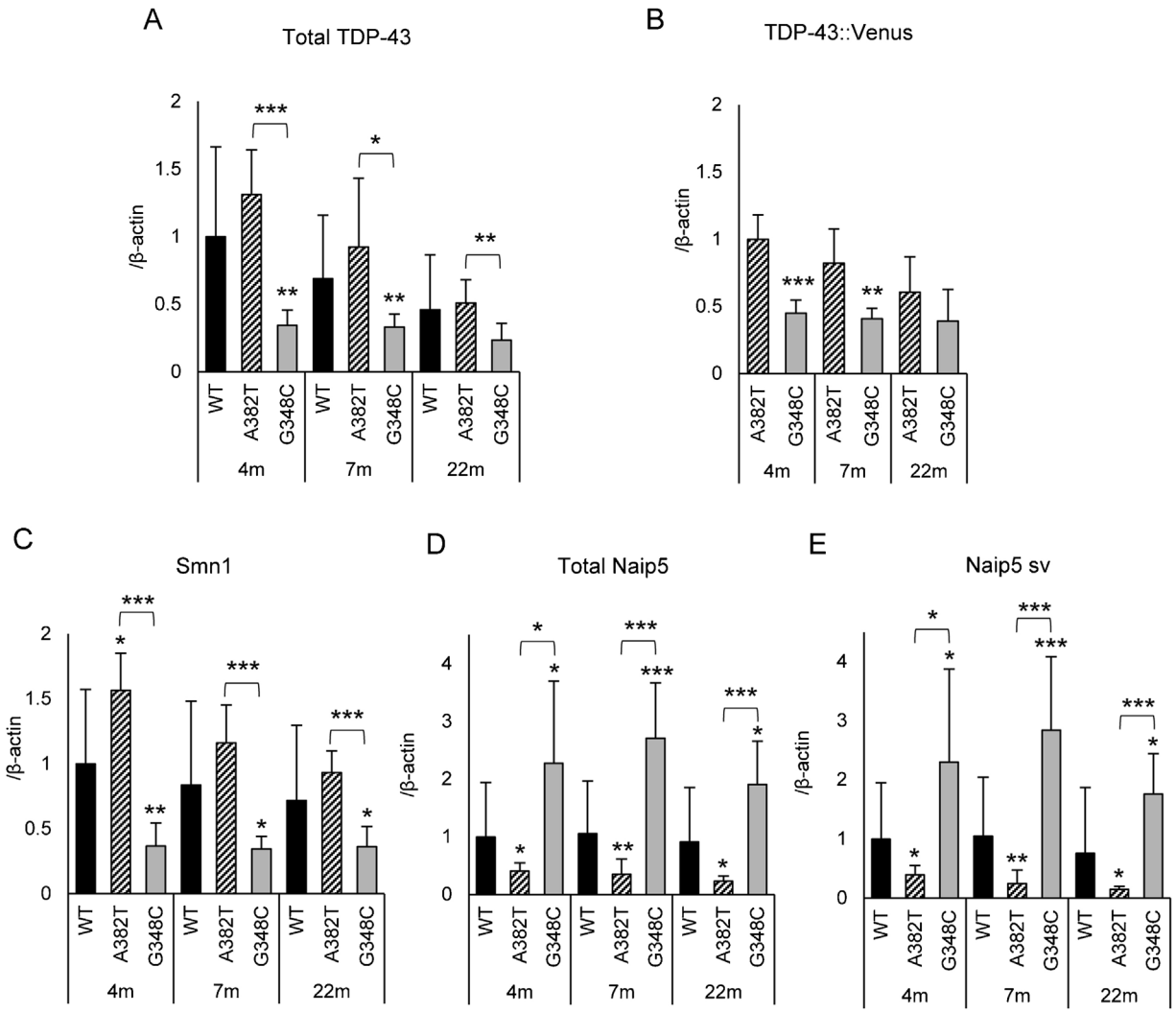

Fig. 6. Changes in RNA metabolism in the WBCs of mutant TDP-43 KI mice. (A–E) Real-time RT-PCR analysis of mutant TDP-43 KI mice WBCs at 4–22 months of age. mRNA expression levels detected by TaqMan® MGB probes binding total TDP-43 (A) and mutant TDP-43 (B). (A) Total TDP-43 mRNA expression was decreased in G348C at 4–22 month old mice relative to those in WT and A382T. Relative to WT: G348C, 0.34 (SD = 0.11), $p = 0.004$ (4 months); 0.33 (SD = 0.10), $p = 0.009$ (7 months), 0.23 (SD = 0.13), $p > 0.05$ (22 months). Relative to A382T: $p = 0.00003$ (4 months), $p = 0.013$ (7 months), $p = 0.002$ (22 months). A382T relative to WT: 1.31 (SD = 0.33; 4 months); 0.92 (SD = 0.51; 7 months); 0.51 (SD = 0.17; 22 months). Total TDP-43 probe was targeted to common sequences of mouse and mutant human TDP-43. (B) Mutant TDP-43 mRNA expression was decreased in G348C relative to that of A382T. G348C, 0.45 (SD = 0.10), $p = 0.0000007$ (4 months); 0.41 (SD = 0.08), $p = 0.002$ (7 months); 0.39 (SD = 0.24), $p > 0.05$. Transgene mRNA was detected by probes designed for Venus sequences. (C–E) mRNA expression of Smn1 (C) and Naip5 (D, E), known to be related to MN survival and anti-apoptotis. In Smn1, relative to WT: G348C, 0.37 (SD = 0.18), $p = 0.002$ (4 months); 0.34 (SD = 0.09), $p = 0.048$ (7 months); 0.36 (SD = 0.16), $p = 0.034$ (22 months). Relative to A382T: $p = 0.0000003$ (4 months); $p = 0.00005$ (7 months), $p = 0.000006$ (22 months). A382T relative to WT: 1.57 (SD = 0.29), $p = 0.018$ (4 months); 1.16 (SD = 0.29), $p > 0.05$ (7 months); 0.93 (SD = 0.17) $p > 0.05$ (22 months). (D) Total Naip5 detected by a probe set into non-exon skipping sequences. Relative to WT: G348C, 2.27 (SD = 1.43), $p = 0.027$ (4 months); 2.71 (SD = 0.96), $p = 0.0005$ (7 months); 1.91 (SD = 0.75), $p = 0.05$ (22 months). Relative to A382T: $p = 0.013$ (4 months), $p = 0.00015$ (7 months), $p = 0.00037$ (22 months). A382T relative to WT: 0.41 (SD = 0.14), $p = 0.046$ (4 months), 0.35 (SD = 0.26), $p = 0.0094$ (7 months); 0.23 (SD = 0.093), $p = 0.012$ (22 months). (E) Naip5 splice variant (sv) was performed by targeting the exon10 and 12 junction. Relative to WT: G348C, 2.30 (SD = 1.57), $p = 0.032$ (4 months); 2.84 (SD = 1.24), $p = 0.0009$ (7 months); 1.76 (SD = 0.69), $p = 0.031$ (22 months). Relative to A382T: $p = 0.018$ (4 months), $p = 0.00052$ (7 months), and $p = 0.00029$ (22 months). A 382 T relative to WT: 0.39 (SD = 0.15) $p = 0.043$ (4 months); 0.25 (SD = 0.22), $p = 0.0071$, (7 months); 0.15 (SD = 0.051), $p = 0.045$ (22 months). N = 13, 15, and 16 in WT; N = 8, 8, and 8 in A382T; N = 7, 8, and 8 in G348C (4, 7, and 22 months). Data were analyzed using an unpaired t-test ($^{*}p < 0.05$, $^{**}p < 0.01$, $^{***}p < 0.001$).

G348C astrocytes (Fig. 2E). Recently, non-cell autonomous signal from glial cells were thought to be related with neurodegeneration in ALS. For example, overexpression of ALS associated mutant TDP-43 driven by an astrocytic promoter was sufficient to cause motor neuron degeneration in rats and was also associated with activation of astrocytes (Tong et al., 2013). Thus, we selected astrocytes in CNS analysis because the cells may play a key role in TDP-43 pathology. And then, we also examined mRNA levels of total, mutant and mouse TDP-43 in brain cortex of the KI mice (Fig. S5). The mRNA levels were not corresponding to protein level completely, but higher in A382T than G348C (Fig. 2 and Fig. S5). It is surprising that protein functions can differ so significantly as a result of substitution of only two amino acids.

To further understand these differences, we investigated the regulation of the two TDP-43 mutants in KI mice astrocytes. In KD experiments, the reduction of mutant human TDP-43 induced an increase in normal TDP-43, and total TDP-43 level was constantly regulated. In contrast, when the total expression level was reduced with WT mouse TDP-43 siRNA, neither TDP-43 mutant showed an increased expression level (Fig. 3). Mutant TDP-43 may thus at least be quantitatively recognized as TDP-43 protein, but neither TDP-43 mutant worked to adjust the total expression level. This response was marked and the difference between normal TDP-43 and TDP-43 mutants associated with the regulation of RNA metabolism and protein expression. Alternatively, this response may be in part related to the lack of 3′UTR TDP-43 mutants. It has previously been

shown that TDP-43 expression is auto-regulated by feedback mechanisms *via* its own 3′UTR (Ayala et al., 2011; Polymenidou et al., 2011; Avendaño-Vázquez et al., 2012). Our experiments show the differences between two mutants occurred in the absence of 3′UTR, indicating that the expression state of TDP-43 is regulated not only via 3′UTR but also each amino acid substitution in the C-terminal domain of TDP-43, e.g. depending on protein half-life the mutant proteins. We note that the TDP-43 mutant mouse model reported here was critical to this discovery.

We then hypothesized that the different expression patterns of the two TDP-43 mutants occurred in peripheral blood (Fig. 4). The protein levels in the A382T mutant were significantly higher than those in G348C, and this result is consistent with those presented above (Fig. 5A). In addition, high non-uniformity of transgene expression was found in A382T mutant WBCs. Although more molecular biological investigations of this non-uniformity are required, the expression states of TDP-43 may be similar between CNS and WBCs. In one previous study, mislocalization of TDP-43 was observed in circulating lymphomonocytes of ALS patients, thus confirming our present results (De Marco et al., 2011). Taken together, we believe that these CNS phenomena can be detected in WBCs and can be used as biomarkers in ALS diagnosis.

To assess the clinical meaning of our results, we analyzed fluorescent signals detected by TDP-43 antibody in WBCs in WT mice. We attempted neurodegenerative diagnosis by performing an imaging study of WBCs for the first time. We characterized TDP-43 expression patterns by modifying the TV lens system of a microscope and using imaging software (Figs. 4 and 5). In A382T mutant mice at the presymptomatic stage, the total TDP-43 expression levels were higher than those in WT and G348C mice (Fig. 5B). In addition, the cell localization of TDP-43 was highly dispersed in A382T only (Fig. 5C and D). Taken together, our results suggest that these phenomena are associated with an abnormality in TDP-43 metabolism in WBCs. In addition, these abnormal states of TDP-43 may differ between mutational positions, which may have caused confusions in the development of biomarkers of ALS diagnosis in the past.

In recent investigations, abnormal RNA metabolism was found to be associated with neurodegeneration (Linder et al., 2015). Furthermore, several previous reports have shown RNA metabolism in peripheral blood. For example, microarray analysis was performed using peripheral blood mononuclear cells of ALS patients, and a number of biomarker candidates were proposed (Mougeot et al., 2011). Additionally, some have focused on microRNA accumulations. For instance, miR-1234-3p and miR-1825 have been found to be downregulated in the serum of ALS patients (Freischmidt et al., 2015). To detect abnormalities in whole blood cells, we investigated mRNA expression of biomarker candidates using WBCs of KI mice. Similar to what was observed on imaging of WBCs (Fig. 5), mRNA expression of A382T was higher than G348C in WBCs (Fig. 6B). Changes in the metabolism of TDP-43 in the CNS may thus also be observed in WBCs.

We focused on MN degenerative factors that have been reported to regulate MN survival and anti-apoptosis. We examined mRNA metabolism of the two mutant human TDP-43 in WBCs of KI mice. SMN protein was found to be ubiquitously expressed in various tissues, including WBCs, but its level was particularly high in MNs (Pellizzoni et al., 1998). The protein functions in the cytoplasmic assembly of snRNP particles that form spliceosomes (Pellizzoni et al., 1998). As shown in a recent study, SMN protein is co-regulated with TDP-43 (Tsuiji et al., 2013). Reflecting this, SMN mRNA levels were consistent with those of total TDP-43 in the WBCs of our KI mice (Fig. 6A and C). Smn1 was not included as a candidate in the TDP-43 KD transcription assay, whereas mRNA of Smn1 decreased in the FUS/TLS KD transcription assay (Lagier-Tourenne et al., 2012). It has been reported that the transcription of Smn1 is regulated by FUS/TLS. These findings suggest that Smn1 expression may be related to the pathology of ALS caused by TDP-43 and FUS/TLS. Notably, we demonstrated that fluctuations in Smn1 expression arise in WBC of ALS model mice. Another interesting factor is NAIP, a member of the Inhibitor of Apoptosis Protein gene family. The protein has also been shown to be ubiquitously expressed with high levels in the CNS, and functions as an apoptosis suppressor that blocks the activities of caspase-3 and caspase-7 (Robertson et al., 2000). NAIP has previously been reported to suppress MN death in an ALS mouse model (mutant SOD1 expressing transgenic mice) (Tanaka et al., 2014). In our KI mice, NAIP mRNA levels were opposite to that of SMN and total TDP-43 (Figs. 6A, C and D). Naip5 was not a candidate of RIP-seq of FUS/TLS, while mRNA of Naip2 has been reported to function as a binding molecule to FUS/TLS (Colombrita et al., 2012). It is thought, including our result, both of Naip2 and Naip5 which were included in the Lgn1 locus related to immunoreaction (Diez et al., 2003) could be useful biomarkers of ALS pathology. Naip5 may be an especially useful biomarker in ALS model mice, given its high levels of expression in WBC compared to other Naip family members. These results suggest that Smn1 and human Naip may also serve as useful biomarkers of human ALS. Our findings may imply that two factors are associated with the MN degenerative response to changes in total TDP-43 expression. Moreover, responses were different between A382T and G348C mutant TDP-43 KI mice, which may have been caused by mutant TDP-43 expression level. To investigate regulation of TDP-43, a splice variant of NAIP was examined at the transcriptional level (Fig. 6E). Although we failed to detect changes using the ratio of splice variants to NAIP, it is possible that an unknown factor causes the accumulation of abnormal splice variants, leading to aberrant RNA metabolism following neurodegeneration. In addition, the two MN degeneration-related factors are known to play crucial roles in spinal muscular atrophy (SMA) pathology (Lefebvre et al., 1995; Roy et al., 1995). It has been proposed that the mechanisms underlying ALS and SMA are linked (Tsuiji et al., 2013). Consequently, it is possible that the metabolism of SMN and NAIP could be used to detect MN degeneration.

Taking a molecular cell biology perspective, we next focused on apoptosis mechanisms, which have been reported to be associated with TDP-43, SMN, and NAIP. Although apoptosis is induced by several stimuli, most activated apoptosis signals are ultimately consolidated in the same pathway and thus these factors may be involved in part of the pathway. TDP-43 is known to regulate expression of Bcl-2 protein, which is a well-known cell death-modulating factor (Sephton et al., 2011). Caspase-9, an apoptosis inducer, is activated by Bcl-2 and leads to the activation of caspase-3, which is known to be an apoptosis effector (Ulukaya et al., 2011). The SMN protein also interacts with Bcl-2 and enhances apoptotic activity (Iwahashi et al., 1997). We performed an exon array analysis in WBCs of KI mice and found that the mRNA level of NAIP differed between WT and A382T mutant mice (Fig. S6). Although the binding mechanism is unclear, NAIP may be regulated by TDP-43 and enhance dysfunction of the apoptotic pathway. In a previous report, mutant TDP-43 (M337V) was found to enhance the levels of cleaved caspase-3 (Mutihac et al., 2015). This suggests that the dysfunction of intracellular signaling associated with mutant TDP-43 may occur at various stages of apoptosis. We have detected the molecular biological symptoms of cell death in WBCs.

We show that the MN death pathway is related to the function of RNA regulation and may be detectable in WBCs. At present, the function of TDP-43 in RNA regulation is being investigated by many groups. For example, non-sense-mediated decay has been shown to occur after deleting a part of the non-coding exon of TDP-43 (Polymenidou et al., 2011). Furthermore, aberration of the TDP-43 splice variant has been reported in the spinal cords of ALS patients (Xiao et al., 2015). Taken together, these results suggest

that TDP-43-related abnormal RNA metabolism could be used as a marker of neurodegeneration.

In conclusion, we find that a combination of TDP-43 and an MN degeneration factors can be used to reflect abnormal RNA metabolism in WBCs and thus be useful as ALS-onset biomarkers. Our results strongly suggest that a combination of candidate biomarkers can detect aberrations in RNA levels in ALS patients. This approach may be useful in neurodegenerative biomarker development.

Acknowledgments

We are grateful to Keiko Bono for technical support of blood collection from heart of mice, and Prof. Douglas Sipp for editing the English of the manuscript. This work was supported by a Grant-in-Aid of The Ishidu Shun Memorial Scholarship, The Tokyo Biochemical Research Foundation Scholarship, MEXT KAKENHI Grant Number 24300122, 25870754, 26111723, and The Jikei University Strategic Prioritizing Research Fund to Hirotaka James Okano. A part of this work was carried out by the Strategic Research Program for Brain Sciences and the Brain Mapping by Integrated Neurotechnologies for Disease Studies (Brain/MINDS) by the Ministry of Education, Culture, Sports, Science and Technology (MEXT) of Japan and Japan Agency for Medical Research and Development (A-MED) to Hideyuki Okano. Hideyuki Okano is a paid Scientific Board of SanBio Co Ltd.

Appendix A. Supplementary data

Supplementary data associated with this article can be found, in the online version, at http://dx.doi.org/10.1016/j.neures.2015.11.009.

References

Arai, T., Hasegawa, M., Akiyama, H., Ikeda, K., Nonaka, T., Mori, H., Mann, D., Tsuchiya, K., Yoshida, M., Hashizume, Y., Oda, T., 2006. TDP-43 is a component of ubiquitin-positive tau-negative inclusions in frontotemporal lobar degeneration and amyotrophic lateral sclerosis. Biochem. Biophys. Res. Commun. 351, 602–611.

Avendaño-Vázquez, S.E., Dhir, A., Bembich, S., Buratti, E., Proudfoot, N., Baralle, F.E., 2012. Autoregulation of TDP-43 mRNA levels involves interplay between transcription, splicing, and alternative polyA site selection. Genes Dev. 26 (15), 1679–1684.

Ayala, Y.M., De Conti, L., Avendaño-Vázquez, S.E., Dhir, A., Romano, M., D'Ambrogio, A., Tollervey, J., Ule, J., Baralle, M., Buratti, E., Baralle, F.E., 2011. TDP-43 regulates its mRNA levels through a negative feedback loop. EMBO J. 30 (2), 277–288.

Buratti, E., Dörk, T., Zuccato, E., Pagani, F., Romano, M., Baralle, F.E., 2001. Nuclear factor TDP-43 and SR proteins promote in vitro and in vivo CFTR exon 9 skipping. EMBO J. 20 (7), 1774–1784.

Chiò, A., Calvo, A., Mazzini, L., Cantello, R., Mora, G., Moglia, C., Corrado, L., D'Alfonso, S., Majounie, E., Renton, A., Pisano, F., Ossola, I., Brunetti, M., Traynor, B.J., Restagno, G., 2012. Extensive genetics of ALS: a population-based study in Italy. Neurology. 79 (19), 1983–1989.

Colombrita, C., Onesto, E., Megiorni, F., Pizzuti, A., Baralle, F.E., Buratti, E., Silani, V., Ratti, A., 2012. TDP-43 and FUS RNA-binding proteins bind distinct sets of cytoplasmic messenger RNAs and differently regulate their post-transcriptional fate in motoneuron-like cells. J. Biol. Chem. 287 (19), 15635–15647.

Corrado, L., Ratti, A., Gellera, C., Buratti, E., Castellotti, B., Carlomagno, Y., Ticozzi, N., Mazzini, L., Testa, L., Taroni, F., Baralle, F.E., Silani, V., D'Alfonso, S., 2009. High frequency of TARDBP gene mutations in Italian patients with amyotrophic lateral sclerosis. Hum. Mutat. 30 (4), 688–694.

De Marco, G., Lupino, E., Calvo, A., Moglia, C., Buccinnà, B., Grifoni, S., Ramondetti, C., Lomartire, A., Rinaudo, M.T., Piccinini, M., Giordana, M.T., Chiò, A., 2011. Cytoplasmic accumulation of TDP-43 in circulating lymphomonocytes of ALS patients with and without TARDBP mutations. Acta Neuropathol. 121 (5), 611–622.

Deng, H.X., Chen, W., Hong, S.T., Boycott, K.M., Gorrie, G.H., Siddique, N., Yang, Y., Fecto, F., Shi, Y., Zhai, H., Jiang, H., Hirano, M., Rampersaud, E., Jansen, G.H., Donkervoort, S., Bigio, E.H., Brooks, B.R., Ajroud, K., Sufit, R.L., Haines, J.L., Mugnaini, E., Pericak-Vance, M.A., Siddique, T., 2011. Mutations in UBQLN2 cause dominant X-linked juvenile and adult-onset ALS and ALS/dementia. Nature 477 (7363), 211–215.

Diez, E., Lee, S.H., Gauthier, S., Yaraghi, Z., Tremblay, M., Vidal, S., Gros, P., 2003. Birc1e is the gene within the Lgn1 locus associated with resistance to *Legionella pneumophila*. Nat. Genet. 33 (1), 55–60.

Droppelmann, C.A., Campos-Melo, D., Ishtiaq, M., Volkening, K., Strong, M.J., 2014. RNA metabolism in ALS: when normal processes become pathological? Amyotroph. Lateral Scler. Frontotemporal Degener. 15 (5–6), 321–336.

Freischmidt, A., Müller, K., Zondler, L., Weydt, P., Mayer, B., von Arnim, C.A., Hübers, A., Dorst, J., Otto, M., Holzmann, K., Ludolph, A.C., Danzer, K.M., Weishaupt, J.H., 2015. Serum microRNAs in sporadic amyotrophic lateral sclerosis. Neurobiol. Aging 9 (36), 2660.e15–2660.e20.

Gitcho, M.A., Baloh, R.H., Chakraverty, S., Mayo, K., Norton, J.B., Levitch, D., Hatanpaa, K.J., White 3rd, C.L., Bigio, E.H., Caselli, R., Baker, M., Al-Lozi, M.T., Morris, J.C., Pestronk, A., Rademakers, R., Goate, A.M., Cairns, N.J., 2008. TDP-43 A315T mutation in familial motor neuron disease. Ann. Neurol. 63 (4), 535–538.

Iwahashi, H., Eguchi, Y., Yasuhara, N., Hanafusa, T., Matsuzawa, Y., Tsujimoto, Y., 1997. Synergistic anti-apoptotic activity between Bcl-2 and SMN implicated in spinal muscular atrophy. Nature 390 (6658), 413–417.

Kabashi, E., Valdmanis, P.N., Dion, P., Spiegelman, D., McConkey, B.J., Vande Velde, C., Bouchard, J.P., Lacomblez, L., Pochigaeva, K., Salachas, F., Pradat, P.F., Camu, W., Meininger, V., Dupre, N., Rouleau, G.A., 2008. TARDBP mutations in individuals with sporadic and familial amyotrophic lateral sclerosis. Nat. Genet. 40, 572–574.

Kabashi, E., Lin, L., Tradewell, M.L., Dion, P.A., Bercier, V., Bourgouin, P., Rochefort, D., Bel Hadj, S., Durham, H.D., Vande Velde, C., Rouleau, G.A., Drapeau, P., 2010. Gain and loss of function of ALS-related mutations of TARDBP (TDP-43) cause motor deficits in vivo. Hum. Mol. Genet. 15 (194), 671–683.

Kwiatkowski Jr., T.J., Bosco, D.A., Leclerc, A.L., Tamrazian, E., Vanderburg, C.R., Russ, C., Davis, A., Gilchrist, J., Kasarskis, E.J., Munsat, T., Valdmanis, P., Rouleau, G.A., Hosler, B.A., Cortelli, P., de Jong, P.J., Yoshinaga, Y., Haines, J.L., Pericak-Vance, M.A., Yan, J., Ticozzi, N., Siddique, T., McKenna-Yasek, D., Sapp, P.C., Horvitz, H.R., Landers, J.E., Brown Jr., R.H., 2009. Mutations in the FUS/TLS gene on chromosome 16 cause familial amyotrophic lateral sclerosis. Science 323 (5918), 1205–1208.

Lagier-Tourenne, C., Polymenidou, M., Hutt, K.R., Vu, A.Q., Baughn, M., Huelga, S.C., Clutario, K.M., Ling, S.C., Liang, T.Y., Mazur, C., Wancewicz, E., Kim, A.S., Watt, A., Freier, S., Hicks, G.G., Donohue, J.P., Shiue, L., Bennett, C.F., Ravits, J., Cleveland, D.W., Yeo, G.W., 2012. Divergent roles of ALS-linked proteins FUS/TLS and TDP-43 intersect in processing long pre-mRNAs. Nat. Neurosci. 15 (11), 1488–1497.

Lefebvre, S., Bürglen, L., Reboullet, S., Clermont, O., Burlet, P., Viollet, L., Benichou, B., Cruaud, C., Millasseau, P., Zeviani, M., 1995. Identification and characterization of a spinal muscular atrophy-determining gene. Cell 80 (1), 155–165.

Linder, B., Fischer, U., Gehring, N.H., 2015. mRNA metabolism and neuronal disease. FEBS Lett. 589 (14), 1598–1606.

Mougeot, J.L., Li, Z., Price, A.E., Wright, F.A., Brooks, B.R., 2011. Microarray analysis of peripheral blood lymphocytes from ALS patients and the SAFE detection of the KEGG ALS pathway. BMC Med Genomic 25 (4), 74.

Mutihac, R., Alegre-Abarrategui, J., Gordon, D., Farrimond, L., Yamasaki-Mann, M., Talbot, K., Wade-Martins, R., 2015. TARDBP pathogenic mutations increase cytoplasmic translocation of TDP-43 and cause reduction of endoplasmic reticulum Ca^{2+} signaling in motor neurons. Neurobiol. Dis. 75, 64–77.

Neumann, M., Sampathu, D.M., Kwong, L.K., Truax, A.C., Micsenyi, M.C., Chou, T.T., Bruce, J., Schuck, T., Grossman, M., Clark, C.M., McCluskey, L.F., Miller, B.L., Masliah, E., Mackenzie, I.R., Feldman, H., Feiden, W., Kretzschmar, H.A., Trojanowski, J.Q., Lee, V.M., 2006. Ubiquitinated TDP-43 in frontotemporal lobar degeneration and amyotrophic lateral sclerosis. Science 314, 130–133.

Pellizzoni, L., Kataoka, N., Charroux, B., Dreyfuss, G., 1998. A novel function for SMN, the spinal muscular atrophy disease gene product, in pre-mRNA splicing. Cell 95 (5), 615–624.

Polymenidou, M., Lagier-Tourenne, C., Hutt, K.R., Huelga, S.C., Moran, J., Liang, T.Y., Ling, S.C., Sun, E., Wancewicz, E., Mazur, C., Kordasiewicz, H., Sedaghat, Y., Donohue, J.P., Shiue, L., Bennett, C.F., Yeo, G.W., Cleveland, D.W., 2011. Long pre-mRNA depletion and RNA missplicing contribute to neuronal vulnerability from loss of TDP-43. Nat. Neurosci. 14 (4), 459–468.

Pradat, P.F., El Mendili, M.M., 2014. Neuroimaging to investigate multisystem involvement and provide biomarkers in amyotrophic lateral sclerosis. Biomed. Res. Int. 2014, 467560.

Renton, A.E., Majounie, E., Waite, A., Simón-Sánchez, J., Rollinson, S., Gibbs, J.R., Schymick, J.C., Laaksovirta, H., van Swieten, J.C., Myllykangas, L., Kalimo, H., Paetau, A., Abramzon, Y., Remes, A.M., Kaganovich, A., Scholz, S.W., Duckworth, J., Ding, J., Harmer, D.W., Hernandez, D.G., Johnson, J.O., Mok, K., Ryten, M., Trabzuni, D., Guerreiro, R.J., Orrell, R.W., Neal, J., Murray, A., Pearson, J., Jansen, I.E., Sondervan, D., Seelaar, H., Blake, D., Young, K., Halliwell, N., Callister, J.B., Toulson, G., Richardson, A., Gerhard, A., Snowden, J., Mann, D., Neary, D., Nalls, M.A., Peuralinna, T., Jansson, L., Isoviita, V.M., Kaivorinne, A.L., Hölttä-Vuori, M., Ikonen, E., Sulkava, R., Benatar, M., Wuu, J., Chiò, A., Restagno, G., Borghero, G., Sabatelli, M., ITALSGEN Consortium, Heckerman, D., Rogaeva, E., Zinman, L., Rothstein, J.D., Sendtner, M., Drepper, C., Eichler, E.E., Alkan, C., Abdullaev, Z., Pack, S.D., Dutra, A., Pak, E., Hardy, J., Singleton, A., Williams, N.M., Heutink, P., Pickering-Brown, S., Morris, H.R., Tienari, P.J., Traynor, B.J., 2011. A hexanucleotide repeat expansion in C9ORF72 is the cause of chromosome 9p21-linked ALS-FTD. Neuron. 72 (2), 257–268.

Robertson, G.S., Crocker, S.J., Nicholson, D.W., Schulz, J.B., 2000. Neuroprotection by the inhibition of apoptosis. Brain Pathol. 10 (2), 283–292.

Rosen, D.R., Siddique, T., Patterson, D., Figlewicz, D.A., Sapp, P., Hentati, A., Donaldson, D., Goto, J., O'Regan, J.P., Deng, H.X., 1993. Mutations in Cu/Zn superoxide dismutase gene are associated with familial amyotrophic lateral sclerosis. Nature 362 (6415), 59–62.

Rowland, L.P., Shneider, N.A., 2001. Amyotrophic lateral sclerosis. N. Engl. J. Med. 344 (22), 1688–1700.

Roy, N., Mahadevan, M.S., McLean, M., Shutler, G., Yaraghi, Z., Farahani, R., Baird, S., Besner-Johnston, A., Lefebvre, C., Kang, X., 1995. The gene for neuronal apoptosis inhibitory protein is partially deleted in individuals with spinal muscular atrophy. Cell 80 (1), 167–178.

Sephton, C.F., Cenik, C., Kucukural, A., Dammer, E.B., Cenik, B., Han, Y., Dewey, C.M., Roth, F.P., Herz, J., Peng, J., Moore, M.J., Yu, G., 2011. Identification of neuronal RNA targets of TDP-43-containing ribonucleoprotein complexes. J. Biol. Chem. 286 (2), 1204–1215.

Sreedharan, J., Blair, I.P., Tripathi, V.B., Hu, X., Vance, C., Rogelj, B., Ackerley, S., Durnall, J.C., Williams, K.L., Buratti, E., Baralle, F., de Belleroche, J., Mitchell, J.D., Leigh, P.N., Al-Chalabi, A., Miller, C.C., Nicholson, G., Shaw, C.E., 2008. TDP-43 mutations in familial and sporadic amyotrophic lateral sclerosis. Science 319, 1668–1672.

Swarup, V., Phaneuf, D., Bareil, C., Robertson, J., Rouleau, G.A., Kriz, J., Julien, J.P., 2011. Pathological hallmarks of amyotrophic lateral sclerosis/frontotemporal lobar degeneration in transgenic mice produced with TDP-43 genomic fragments. Brain 134 (9), 2610–2626.

Tanaka, K., Kanno, T., Yanagisawa, Y., Yasutake, K., Inoue, S., Hirayama, N., Ikeda, J.E., 2014. A novel acylaminoimidazole derivative, WN1316, alleviates disease progression via suppression of glial inflammation in ALS mouse model. PLoS ONE 9 (1), e87728.

Tarasiuk, J., Kułakowska, A., Drozdowski, W., Kornhuber, J., Lewczuk, P., 2012. CSF markers in amyotrophic lateral sclerosis. J. Neural Transm. 119 (7), 747–757.

Tong, J., Huang, C., Bi, F., Wu, Q., Huang, B., Liu, X., Li, F., Zhou, H., Xia, X.G., 2013. Expression of ALS-linked TDP-43 mutant in astrocytes causes non-cell-autonomous motor neuron death in rats. EMBO J. 32 (13), 1917–1926.

Tsuiji, H., Iguchi, Y., Furuya, A., Kataoka, A., Hatsuta, H., Atsuta, N., Tanaka, F., Hashizume, Y., Akatsu, H., Murayama, S., Sobue, G., Yamanaka, K., 2013. Spliceosome integrity is defective in the motor neuron diseases ALS and SMA. EMBO Mol Med 5 (2), 221–234.

Ulukaya, E., Acilan, C., Yilmaz, Y., 2011. Apoptosis: why and how does it occur in biology? Cell Biochem. Funct. 29 (6), 468–480.

Valadi, N., 2015. Evaluation and management of amyotrophic lateral sclerosis. Prim. Care 42 (2), 177–187.

Watanabe, S., Kaneko, K., Yamanaka, K., 2013. Accelerated disease onset with stabilized familial amyotrophic lateral sclerosis (ALS)-linked mutant TDP-43 proteins. J. Biol. Chem. 288 (5), 3641–3654.

Wu, C.H., Fallini, C., Ticozzi, N., Keagle, P.J., Sapp, P.C., Piotrowska, K., Lowe, P., Koppers, M., McKenna-Yasek, D., Baron, D.M., Kost, J.E., Gonzalez-Perez, P., Fox, A.D., Adams, J., Taroni, F., Tiloca, C., Leclerc, A.L., Chafe, S.C., Mangroo, D., Moore, M.J., Zitzewitz, J.A., Xu, Z.S., van den Berg, L.H., Glass, J.D., Siciliano, G., Cirulli, E.T., Goldstein, D.B., Salachas, F., Meininger, V., Rossoll, W., Ratti, A., Gellera, C., Bosco, D.A., Bassell, G.J., Silani, V., Drory, V.E., Brown Jr., R.H., Landers, J.E., 2012. Mutations in the profilin 1 gene cause familial amyotrophic lateral sclerosis. Nature 488 (7412), 499–503.

Xiao, S., Sanelli, T., Chiang, H., Sun, Y., Chakrabartty, A., Keith, J., Rogaeva, E., Zinman, L., Robertson, J., 2015. Low molecular weight species of TDP-43 generated by abnormal splicing form inclusions in amyotrophic lateral sclerosis and result in motor neuron death. Acta Neuropathol 130 (1), 49–61.

Yokoseki, A., Shiga, A., Tan, C.F., Tagawa, A., Kaneko, H., Koyama, A., Eguchi, H., Tsujino, A., Ikeuchi, T., Kakita, A., Okamoto, K., Nishizawa, M., Takahashi, H., Onodera, O., 2008. TDP-43 mutation in familial amyotrophic lateral sclerosis. Ann. Neurol. 63, 538–542.